Research paper

Size-segregated sulfate on top of Mt. Fuji transported from Sakurajima volcano eruption

Kojiro SHIMADA [1, 5*], Kei SUZUKI [1], Shungo KATO [2], Syuichi ITAHASHI [3, 6] and Shiro HATAKEYAMA[1,4]

[1] Tokyo University of Agriculture and Technology, 3-5-8 Saiwaicho, Fuchu, Tokyo 183-8509, Japan
[2] Tokyo Metropolitan University, Minami-oosawa, Hachioji, Tokyo, 192-0397, Japan
[3] Sustainable System Research Laboratory (SSRL), Central Research Institute of Electric Power Industry (CRIEPI), Abiko, Chiba 270-1194, Japan
[4] Asia Center for Air Pollution Research, Niigata, Sone, Niigata, 950-2144, Japan, 914 Kamitanadare, Kazo, Saitama 347-0115, Japan
[5] Department of Chemistry, Biology, and Marine Science, University of the Ryukyus, Okinawa 903-0213 Japan
[6] Research Institute for Applied Mechanics, Kyushu University, Fukuoka 816-8580 Japan

*Corresponding Author.
E-mail: kshimada@sci.u-ryukyu.ac.jp (K. Shimada)
Tel: 098-895-8526

Abstract

Size-segregated aerosol samples were collected on Mt. Fuji with a cascade impactor during daytime and nighttime. We analyzed for their ionic and element compositions. Samples were collected from 29 July to 2 August (first period) and from 19 to 21 August 2013 (second period). Based on combined chemical components and CMAQ, in the first period, the air masses had been transported from East Asia. In the second period, the Sakurajima volcano eruption had been transported. NH_4^+, $SO_4^{2-}$and elements were the major ions in $2.5 < Dp \leq 10$ during the second period. The slope of a linear regression of non-sea-salt (nss)-SO_4^{2-} versus NH_4^+ was nearly unity, particularly during the first period. However, nss-SO_4^{2-} in coarse aerosol was shifted in great excess in the second period. We have observed a rare phenomenon in which sulfate shifts to $2.5 < Dp \leq 10$. Although the formation process of $(NH_4)_2SO_4$ in coarse particle is hypothesized two mechanisms, we hypothesize the third mechanism in this study. Currently, radiative forcing is being discussed for the detection of volcanic aerosols using satellites with particle sizes of 1.2 μm. If this can be clarified, it will improve the reproducibility of sulfate radiative forcing.

Keywords : Size-segregated aerosol, Size distribution of sulfate, Mt. Fuji, East Asia, Sakurajima volcano eruption

1. Introduction

Transport of aerosols in the free troposphere is of great interest and an important problem with respect to air pollution and volcano eruption transported long range distance (Osada *et al*., 2009). The climate impacts of volcanic aerosols in the troposphere and stratosphere have received attention (Hoffmann *et al*., 2009; Solomon *et al*., 2011). Volcanic eruptions have continuously increased stratospheric aerosol levels (Wu *et al*., 2023). Japan, in particular, is a region with many volcanoes, and the frequency of volcanic eruptions is increasing. In that case, it is essential to accurately estimate the climate impacts of volcanic eruptions because the climate impact of anthropogenic greenhouse gases and aerosol particles could be better assessed if natural forcings, such as volcanic eruptions, are explicit (Wu *et al*., 2023).

The atmospheric background conditions, the amount of emitted SO_2, and the plume heights of volcanic eruptions are all essential parameters that directly determine the transport pathways of volcanic SO_2 and sulfate aerosols (Wu *et al*. 2023). There are few 3000m-class observation sites in Asia. Mt. Fuji is one of the few observation sites in the 3000m a.s.l class (Okamoto *et al*., 2016). Mt. Fuji is an isolated peak with a sharp, symmetric shape similar to an artificial tower (Kaneyasu *et al*., 2007; Wai *et al*., 2008).

Kato *et al*. (2016) previously reported that SO_2 in the plume from the Mt. Sakurajima eruption was observed on at Mt. Fuji in August 2013. The dynamics of chemical speciation, including not only gases but also particles in the plume, have not been clarified. We also measured size-segregated aerosols during our same measurement period.

In mountain sites, the chemical composition of aerosols has scarcely been reported. The aerosol number and mass concentration are mainly investigated for size-segregated aerosol in review paper of mountain measurement sites (Okamoto *et al*., 2016). In the work reported here, therefore, we showed that ionic and element compositions in size-segregated aerosols including aerosol mass concentration transported East Asia and Sakurajima volcano eruption. In particular, we reported on characteristic of distribution of sulfates in Sakurajima volcanic plumes transported long range distance to Mt. Fuji in free troposphere.

2. Experimental Methods

2.1 Size-segregated Aerosol Sampling on the Top of Mt. Fuji

Observations were carried out at the Mt. Fuji Research Station (35.36°N, 138.73°E, 3776 m a.s.l.) in summer 2013 (Shimada *et al*. 2024; Kato *et al*., 2016). The pressure pattern in summer is located over the western Pacific Ocean, generally (Miura *et al.* 2019). Size-segregated sampling of aerosols was carried out from 18:00 JST 29 July to 6:00 JST 2 August 2013 (first period) and from 18:00 JST 19 August to 6:00 JST 21 August 2013 (second period). Each sample was collected for 12 hours from 18:00 on one day to 6:00 on the next day (nighttime sample) during valley wind in troposphere, and from 6:00 to 18:00 (daytime sample) during mountain wind in free troposphere.

Sampling was carried out with a five-stage cascade impactor (Nanosampler Model 3180, KANOMAX JAPAN Inc., Osaka, Japan). Aerosols with a particle diameter (Dp) in five size ranges, $Dp \leq 0.5$ μm, $0.5 < Dp \leq 1$ μm, $1 < Dp \leq 2.5$ μm, $2.5 < Dp \leq 10$ μm and 10 μm < Dp were collected on polytetrafluoroethylene filters with a diameter of 55 mm (PF020, ADVANTEC, Tokyo, Japan) (Shimada *et al*. 2024).

A Nanosampler was set up in the 3rd building of the Mt. Fuji Observatory (the Mount Fuji Research Station). The inlet of a high-volume air sampler was placed on the ground floor of the same building to draw in outside air at a flow rate of 1000 L/min. Outside air was sampled with a dry diaphragm vacuum pump (DA-121D, ULVAC Inc., Tokyo, Japan; maximum flow rate 120 L/min) under the control of a mass flow controller (Model8550, KOFLOC Inc., Kyoto, Japan) set at 40 L/min (Shimada *et al*. 2024). Filters were weighed before and after sampling with an ultra-micro balance (UMX2, Mettler Toledo International Inc., Tokyo, Japan) to determine the mass concentrations of particles in each size range.

Back trajectories of particles at the top of Mt. Fuji (35.36°N, 138.73°E, 3776 m a.s.l.) were calculated for 96 hours from 18:00 (nighttime sample) and 6:00 (daytime sample) by using the HYbrid Single-Particle Lagrangian Integrated Trajectory (HYSPLIT) model on the National Oceanic and Atmospheric Administration (NOAA) web site (Stein *et al*. 2015).

To identify Mt. Sakurajima eruption and Asian outflow by simulation model, Community Multiscale Air Quality Modeling System (CMAQ) version 5.3.3 (U.S. Environmental Protection Agency, 2021) was used. The SO_2 emission from 16 Japanese

volcanoes were obtained from the Japan Meteorological Agency (Japan Meteorological Agency, 2024) and the anthropogenic emissions were taken from the Hemispheric Transport of Air Pollution version 3 (HTAP_v3) dataset (Crippa *et al*. 2023). The gas and aerosol chemistry modules used in the CMAQ model were SAPRC07tic (Xie *et al*. 2013) and aero7 (Xu *et al*. 2018), respectively. To improve the modeling of SO_4^{2-} oxidation process, the aqueous-phase SO_4^{2-} formation from SO_2 and NO_2 (Itahashi *et al*. 2021) and the enhancement of iron solubility in the aqueous-phase SO_4^{2-} reaction in O_2 oxidation catalyzed by transition-metal ions (Itahashi *et al*. 2022) were included with the Transition Metal Inventory-Asia version 1.0 (Kajino *et al*. 2020). The details of modeling design and applications for volcanoes and the long-range transport were found in our previous studies (e.g., Itahashi *et al*. 2019; 2023). In this study, CMAQ simulation was started from 1 July 2013, and we analyzed the model results for first and second periods. The impact of 16 Japanese volcanoes was evaluated by switching off SO_2 emission from 16 Japanese volcanoes, and the impact of Sakurajima was additionally evaluated by switching off SO_2 emissions from Sakurajima.

2.2 Analyses of ionic species

Each sampling filter was then cut into two pieces, one of which was analyzed for ionic components and the other for elements. The concentrations of ionic species in aerosols were assessed after ultrasonic extraction of components with a mixture of ethanol (100 μL) and distilled water (10 mL) in a polypropylene tube for 20 min. The concentrations of the ions Cl^-, NO_3^-, SO_4^{2-}, Na^+, NH_4^+, K^+, Mg^{2+}, and Ca^{2+} were assessed by ion chromatography (Shimadzu LC10AD, Shimadzu Corporation, Kyoto, Japan). Anions were separated by a column for anions (Shimadzu IC-SA2) and identified with a conductivity detector (Shimadzu CDD-10Asp) with a suppresser. Cations were separated by a column for cations (Shimadzu IC-C4) and identified with a conductivity detector (Shimadzu CDD-6A) but without a suppresser (Shimada *et al*. 2024; Yumoto *et al*., 2015).

The concentrations of elements in aerosols were quantitatively assessed after digestion of components with a mixture of 1.5 mL HF (Wako Pure Chemical Industries, Ltd.,

Osaka, Japan), 2.5 mL HNO_3 (Kanto Chemical Co., Inc., Tokyo, Japan), and 0.5 mL H_2O_2 (Wako) in a Teflon vessel placed in a microwave oven operated at 200 W for 10 min. After digestion, the HF was removed by evaporation at 200 °C on a hot plate in a hood. Sample solutions were prepared by the addition of nitric acid followed by filtration. The isotopes ^{7}Li, ^{23}Na, ^{24}Mg, ^{27}Al, ^{39}K, ^{43}Ca, ^{51}V, ^{53}Cr, ^{55}Mn, ^{57}Fe, ^{59}Co, ^{60}Ni, ^{63}Cu, ^{66}Zn, ^{69}Ga, ^{75}As, ^{82}Se, ^{85}Rb, ^{88}Sr, ^{95}Mo, ^{107}Ag, ^{111}Cd, ^{115}In, ^{118}Sn, ^{121}Sb, ^{133}Cs, ^{137}Ba, ^{139}La, ^{205}Tl, ^{208}Pb, and ^{209}Bi were analyzed by inductively coupled plasma mass spectrometry (Agilent 7500, Agilent Technologies, Inc., California, USA) (Shimada *et al*. 2024; Yumoto *et al.*, 2015).

3. Results and Discussion

3.1 Size distribution of aerosols transported from the East Asia, Japan and Sakurajima volcano eruption

Average mass concentrations of Dp ≤ 0.5 μm, 0.5 < Dp ≤ 1 μm, 1 < Dp ≤ 2.5 μm, 2.5 < Dp ≤10 μm and 10 μm < Dp were 1.49 ± 0.43 μg/m^3, 1.09 ± 0.50 μg/m^3, 1.42 ± 0.67 μg/m^3, 1.29 ± 1.72 μg/m^3 and 0.28 ± 0.33 μg/m^3, respectively, in the first period (**Fig. 1**). CMAQ and back trajectories in the first period indicated that the aerosols had come mainly from China and had passed over Korea (**Fig. S1, Fig. S2**). According to Shimada *et al*. (2024), they are investigating that long-range transported air pollution (LRTAP) mixed with domestic air pollution (DAP) during the daytime (D) transported from China to Mt. Fuji are identified based on the proportion of elements in the collected size-segregated aerosols and a combination of backward trajectory analysis and satellite observation CLIPSO. When the contribution of domestic source is high, the proportion of Zn is high. And when the contribution of Chinese source is high, the proportion of Pb is high. Based on the result, we found that the proportion of elements transported over long distances from China at nighttime (N) showed a high proportion of Pb (**Fig. S3**). In this study, we discussed size distributions of aerosols observed in the first period and the second period without separating mountain and valley winds to compare LRTAP (D and N) and DAP with Sakurajima volcano eruption. In **Fig. S2**, CMAQ calculated sulfuric acid concentration within 0-3000m during the daytime and nighttime. On the other hand, during the nighttime, the sulfuric acid concentration on 30 (D) July 2013 was calculated

within 2000-3000m in **Fig. 2**. The contribution of Asian outflow was found to be strong during both daytime periods. CMAQ represented sulfate concentrations by altitude considering mountain and valley winds.

Whereas, in the second period, they were 1.79 ± 0.63 μg/m^3, 1.40 ± 0.67 μg/m^3, 1.96 ± 1.21 μg/m^3, 2.55 ± 2.80 μg/m^3 and 0.56 ± 0.70 μg/m^3, respectively (**Fig. 1**). Sakurajima volcano was active and erupted many times during 17–19 August 2013. A large-scale eruption took place at 16:31 JST 18 August 2013. Kato *et al*. (2016) previously reported that SO_2 in the plume from the Sakurajima volcano eruption was observed during our same measurement period on at Mt. Fuji in 19-21 August 2013 (**Fig. 2**). Back trajectories in the second period showed that the aerosols had passed over the Japanese islands of Kyushu or Shikoku (**Fig. S1**). The contrast between the back trajectories during the two periods was clear. CMAQ, which is the difference in volcanic emissions showed that sulfate concentration was transported to Mt. Fuji from Sakurajima during 19 August to 21 August 2013 (second period) (**Fig. 2**). These findings showed that sulfate was transported to Mt. Fuji (**Fig. 2, Fig. S3**). In **Fig. S4**, CMAQ calculated sulfuric acid concentration within 0-3000m during the daytime and nighttime. On the other hand, during nighttime, the sulfuric acid concentration was calculated within 2000-3000m (**Fig. 2**). The sulfate concentration was low because the edge of the volcanic plume was grazing Mt. Fuji, consistent with atmospheric measurements and CMAQ (**Fig. 2, Fig. S3**). When this study was compared with the high sulfate concentration observed at Noto during the Sakurajima volcanic eruption (Watanabe *et al*. 2015), this study was observed in the edge of the volcanic plume. CMAQ also could represent sulfate concentrations by altitude considering mountain and valley winds. From these results, we found that we were observing Sakurajima volcanic plume both during the daytime and at nighttime.

Average mass concentrations in Dp ≤ 0.5 μm, 0.5 < Dp ≤ 1 μm, 1 < Dp ≤ 2.5 μm, 2.5 < Dp ≤10 μm and 10 μm < Dp during the second period were 1.20, 1.28, 1.38, 1.93 and 2.00 times those in the first period, respectively (**Fig. 1**). Therefore, mass concentrations, particularly those of the larger particles (2.5 < Dp ≤10 μm, 10 μm < Dp), were higher in the second period.

The main ionic component was SO_4^{2-} during both periods (**Fig. 3**). Its average percent contributions in Dp ≤ 0.5 μm, 0.5 < Dp ≤ 1 μm, 1 < Dp ≤ 2.5 μm, 2.5 < Dp ≤10 μm and 10 μm < Dp were 64.9±8.1%, 67.1 ± 3.5%, 68.5 ± 3.2%, 55.9 ± 12.0% and 55.1 ± 11.2%,

respectively, in the first period and 40.7 ± 9.7%,42.9 ± 13.2%,66.3 ± 9.3%, 73.5 ± 9.0%, and 67.1 ± 7.5%, respectively, in the second period. Ionic concentrations peaked in 1 < Dp ≤ 2.5 μm in the first period and in 1 < Dp ≤ 2.5 μm in the second period (**Fig. 3**). The size distribution of the ionic species therefore shifted toward larger particles in the second period. **Figure 4** shows the size distribution of twelve elements (natural source: Mn, Fe, Na, Na, Mg, Al, Anthropogenic source: Bi, Sb, As, Zn, Cu, Pb, V) from among the 16 elements measured in most samples. Similar to sulfate, the distribution of all of elements peaked in 2.5 < Dp ≤10 μm during second period. This indicates that aerosols derived from Sakurajima volcanic eruptions were observed on Mt. Fuji both day and night.

In order to distinguish between anthropogenic and natural sources of elements, we checked the enrichment factor (EF) values of metallic elements. EF values are defined by the following equation.

$$EF_{soil}(X) = \frac{(X/REF)_{aerosol}}{(X/REF)_{crust}} \quad (1)$$

Here, $(X/REF)_{aerosol}$ and $(X/REF)_{crust}$ are the ratios of the concentrations of a target element to a reference element (here Al was chosen as the reference element) in an aerosol and in soil, respectively. We used the average concentrations of elements in soil reported by Taylor *et al*. (1995). EF < 2 suggests mainly natural crustal sources, and EF > 10 suggests strong enrichment from noncrustal sources (Gao et al., 2002).

For example, EF values of V were found to be 5.8–8.7 for Dp ≤ 0.5 μm and 3.4–6.4 for 0.5 < Dp ≤ 1 μm, the implication being that the V, Pb, As etc., in these particles was derived mainly from natural sources. In our previous study (Taniguchi *et al*., 2017; Shimada et al., 2017) at Cape Hedo, Okinawa, we found EF values of V in size-segregated aerosol samples to be ~30 for Dp ≤ 0.5 μm and 130 for 0.5 < Dp ≤ 1 μm. There was thus evidence of a large contribution of anthropogenic components transported from the Asian continent. The V in the aerosols collected at the top of Mt. Fuji, mainly in the second period, was therefore likely of natural source such as from a volcanic eruption. Therefore, it was found that the influence of volcanoes is stronger during the daytime in mountain breeze and nighttime in valley breeze.

3.2 The extent of sulfur oxidation in Sakurajima volcanic plume

To understand the extent of sulfur oxidation in air, we calculated the fraction of oxidized sulfur present as sulfate (*Fs*) with the following equation.

$$Fs = \text{nss-}SO_4^{2-} / (SO_2 + \text{nss-}SO_4^{2-}) \quad (1)$$

The *Fs* value at night on 20 August was 0.58 (**Table S1**). Our CMAQ simulation also showed that *Fs* value was low (**Fig. 2**). On other days, especially in the first period, *Fs* was 0.94-1. The *Fs* value at night on 20 August is much smaller than the value observed at Cape Hedo, Okinawa (0.83, Takami *et al*., 2007; 0.75, Shimada *et al*., 2015), where most of the sulfur in the air is oxidized during long-range transport. CMAQ simulation show that *Fs* value at Cape Hedo is 95.8－99.9% and 63.0% derived from China and Mt. Aso volcanic plume (Itahashi *et al*., 2017). A large amount of SO_2 emitted from Sakurajima volcano eruption therefore arrived at Mt. Fuji before being oxidized. Basically, SO_2 are oxidized by OH radicals to H_2SO_4.

However, a large amount of SO_2 emitted from Sakurajima volcano eruption therefore arrived at Mt. Fuji before being oxidized because based on the reaction rate, OH radicals cannot exist in excess of SO_2. Moreover, Itahashi *et al*. (2017) reported that the temporal variation of the modeled volcano absolute source apportionment and coarse-mode nss-SO_4^{2-} of Dp > 10 μm observed by the size-segregated cascade impactor. They showed moderate correlation (R = 0.64), and both revealed the maximum attribution to the volcano source. They also report that the approach of specifying emission sources both from model and observations is necessary to have confidence in the estimation results. In this study, our results demonstrated reproducibility in estimating volcanic sources.

3.3 Chemical form of SO_4^{2-} in fine and coarse aerosols Ion balance

NH_4^+ and SO_4^{2-} were the major ionic components in the fine (Dp ≤ 0.5 μm, 0.5 < Dp ≤ 1 μm, 1 < Dp ≤ 2.5 μm) and coarse (2.5 < Dp ≤10 μm, 10 μm < Dp) aerosols (**Fig. 5**). They are formed by the neutralization reaction between H_2SO_4 and NH_3 in air (Reaction (1)) and exist as ammonium sulfate ($(NH_4)_2SO_4$) (Yeatman *et al*., 2001; Okuda *et al*.,

2007).

$$H_2SO_4 + 2NH_3 \rightarrow (NH_4)_2SO_4 \quad (1)$$

NH_4^+ was strongly correlated with nss-SO_4^{2-} ($R^2 = 0.72$) in this study. Scatter plots of nss-SO_4^{2-} against NH_4^+ (**Fig. 5**) gave a straight line with a slope of nearly unity, particularly in the first period. This scatter plots based on equivalent concentrations (neq/m^3) can show whether they are formed by the neutralization reaction or not (Yumoto *et al*., 2015). It thus appears that nss-SO_4^{2-} existed as $(NH_4)_2SO_4$ in the first period. It can therefore be inferred that nss- SO_4^{2-} in the first period had been transported mainly from China and Korea.

In contrast, nss-SO_4^{2-} was present in great excess compared to NH_4^+ during the night of 20 August (**Fig. S3**). The excess nss-SO_4^{2-} must have been present as sulfuric acid because, as reported before, high concentrations of SO_2 were observed simultaneously (Kato *et al*., 2016). Scatter plots of nss-SO_4^{2-} against NH_4^+ (**Fig. 5**) gave a straight line with a slope of nearly unity, particularly in the first period. Here, the value obtained by subtracting the total amount of cations from the total amount of anions was defined as infer-H^+. In addition, the excess nss-SO_4^{2-} in that was not bonded to NH_4^+, which is the main counter ion, was designated as ex- SO_4^{2-}.

$$[\text{ex-}SO_4^{2-}] = [\text{nss-}SO_4^{2-}] - [NH_4^+] \quad (2)$$

In the second period, the coefficient of determination between infer-H^+ and ex-SO_4^{2-} was 0.91, indicating a high correlation, suggesting that H^+ in aerosols is related to particles containing nss-SO_4^{2-}. Here, the vertical axis represents the equivalent concentration of nss-SO_4^{2-}, and the horizontal axis represents the equivalent concentration of NH_4^+ + infer-H^+, as shown in **Fig. 5**. It is mainly plotted on y=x, and in the second period, not only $(NH_4)_2SO_4$ but also the production of unneutralized H_2SO_4 is included when the air mass from the Sakurajima volcano eruption is transported to Mt. Fuji.

3.4 $(NH_4)_2SO_4$ in coarse particles

Sulfate aerosols such as $(NH_4)_2SO_4$ usually exist as fine particles. However, SO_4^{2-} existed in coarse particles during the second period (**Fig. 6**). In coarse particles, SO_4^{2-} is usually present as $Ca(SO_4)_2$ (Zhuang *et al*., 1999), but the concentration of Ca^{2+} in the particles was low (**Fig. 4**) in the second period, and the concentration of NH_4^+ was relatively high. The sulfate therefore existed as $(NH_4)_2SO_4$ (**Fig. 5**), with ex-SO_4^{2-} existing as free sulfuric acid.

Yeatman *et al*., (2001) have hypothesized two mechanisms by which coarse $(NH_4)_2SO_4$ particles might be formed: (1) by neutralization of the surface of coarse, acidic particles by gaseous NH_3 (Zhuang *et al*., 1999; Yeatman *et al*., 2001; Parmar *et al*., 2001), and (2) by condensation of fine $(NH_4)_2SO_4$ particles on the surface of coarse particles (Yeatman *et al*., 2001; Xiaoxiu *et al*., 2003).

If the first mechanism is the explanation, then fine particles should be basic, and gaseous NH_3 should be present in large excess (Zhuang *et al*., 1999; Yeatman *et al*., 2001, Parmar *et al*., 2001). In the present case, however, fine particles were not basic, and it is unlikely that NH_3 was present in excess in second period in the free troposphere. Therefore, the first mechanism is not plausible.

Although the element concentrations in coarse particles were high on the night of 19 August and day of 20 August, the element concentration was not high on the night of 20 August (**Fig. S3**). However, the concentration of SO_4^{2-} in coarse particles still was very high (**Fig. S3**) and even included excess sulfuric acid, as described above. It is thus unlikely that $(NH_4)_2SO_4$ condensed on the surfaces of volcanic ash particles during night of 19 August and day of 20 August.

Thus, there will be third mechanism. **Fig. 6** showed the distribution of nss-SO_4^{2-} concentration at Cape Hedo and Tokyo to compare with Mt. Fuji (**Fig. 3**). Yumoto *et al*. (2016) reported that when nss-SO_4^{2-} is transported from China to Cape Hedo for long rang transport, distribution of nss-SO_4^{2-} concentrations were peaked in $0.5 < Dp \leq 1$ μm and $1 < Dp \leq 2.5$ μm due to coagulation process. Moreover, distribution of nss-SO_4^{2-} concentrations were peaked in $0.5 < Dp \leq 1$ μm and $1 < Dp \leq 2.5$ μm at Tokyo in summer due to high humidity (Shimada *et al*. 2021). This is because the distribution of nss-SO_4^{2-} concentration cannot grow until the size range of $0.1 < Dp \leq 0.5$ at Tokyo in winter due

to low humidity (Shimada *et al*. 2021). On other hand, in this study, the distribution of nss-SO_4^{2-} concentrations were peaked in 1 < Dp ≤ 2.5 μm and 2.5 < Dp ≤10 μm.

Because the top of Mt. Fuji is often enveloped in dense fog, fine particles can be captured in fog droplets (Kevin *et al*., 1992; Goran *et al*., 1998). It seems very likely that fine particles were trapped in fog droplets and coagulated as coarse particles. The low mass concentration of the nighttime sample on 20 August also supports this scenario, because fog water is likely to evaporate after particles are collected on filters. However, our report on whether the aerosols are caused by fog or volcanic growth is still only a hypothesis during night of 19 August and day of 20 August. In the future, it will be necessary to examine volcanic plumes using new atmospheric measurement methods to examine the reproducibility of this hypothesis.

5. Conclusions

The size distribution of the mass concentration, ionic and elemental components of aerosols were measured at the top of Mt. Fuji in summer 2013 with a cascade impactor. We observed LRTAP from 29 July to 2 August and a plume from Sakurajima volcano during 19–20 August. A comparison of average mass concentrations during the first period with those in the second period revealed that mass concentrations were higher in the second period, particularly those of particles in 2.5 < Dp ≤10 μm and 10 μm < Dp. Ionic concentrations peaked in 0.5 < Dp ≤ 1 μm and 1 < Dp ≤ 2.5 μm during the first periods. The concentrations of most elements in the second period peaked 2.5 < Dp ≤10 μm. During the second period, a large amount of SO_2 emitted from Mt. Sakurajima arrived at the top of Mt. Fuji before being oxidized. A comparison of the different size distributions of $(NH_4)_2SO_4$ aerosols during the first and the second periods suggested that coarse $(NH_4)_2SO_4$ particles may have formed as a result of fine particles' being trapped in fog droplets and subsequently coagulating as coarse particles. The low mass concentration of the nighttime sample on 20 August also supports this scenario, because fog water is likely to evaporate after particles are collected on filters. However, our report on whether the aerosols are caused by fog or volcanic growth is still only a hypothesis during night of 19 August and day of 20 August. In the future, it will be necessary to examine volcanic plumes using new atmospheric measurement methods to examine the

reproducibility of this hypothesis. This is the first comparison in Asia of volcanic sulfate with a simulation model that takes into account mountain and valley winds and observed values. This study provided important information for predicting climate change due to volcanic eruptions.

Currently, radiative forcing is being discussed for the detection of volcanic aerosols using satellites with particle sizes of 1.2 μm. When combined with a climate change model, the amount of SO_4^{2-} produced is calculated from the amount of SO_2 emission. Sulfate may not show a maximum concentration at 1.2 μm, as in the present study. If this third mechanism is not considered in the simulation model, it will lead to overestimation of sulfate. Therefore, it is necessary to measure chemical components according to particle size distribution. If this can be clarified, it will contribute to improving the reproducibility of sulfate radiative forcing using simulation models.

Acknowledgments

The authors are grateful to the Mount Fuji Research Station NPO (non-profit organization) for keeping and operating the Mt. Fuji observatory. We are also grateful to Prof. Hiroshi Okochi of Waseda University for his help during our experiment. This study was partially supported by the Funding to Environmental NPO from the Hitachi Environment Foundation in 2013.

References

1. Crippa, M., Guizzardi, D., Butler, T., Keating, T., Wu, R., Kaminski, J., Kuenen, J., Kurokawa, J., Chatani, S., Morikawa, T., Pouliot, G., Racine, J., Moran, M. D., Klimont, Z., Manseau, P. M., Mashayekhi, R., Henderson, B. H., Smith, S. J., Suchyta, H., Muntean, M., Solazzo, E., Banja, M., Schaaf, E., Pagani, F., Woo, J. H., Kim, J., Monforti-Ferrario, F., Pisoni, E., Zhang, J., Niemi, D., Sassi, M., Ansari, T., Foley, K.: The HTAP_v3 emission mosaic: merging regional and global monthly emissions (2000-2018) to support air quality modeling and policies, *Earth Syst. Sci. Data*, 15, 2667–2694, doi:10.5194/essd-15-2667-2023 (2023).Gao, Y., Nelson, D.E., Field, P.M., Ding, Q., Li, H., Sherrell, R.M., Gigliotti, C.L., Ryda, V., Glenn, T.R.

Eisenreich, S.J.: Characterization of Atmospheric Trace Elements on PM2.5 Particulate Matter over the New York–New Jersey Harbor Estuary. *Atmos. Environ.*, **36**: 1077–1086, doi: 10.1016/S1352-2310(01) 00381-8, (2002).

2. Goran, F., Bengt, G. M., Sven-Inge, C., Olle, H. B., Erik, S., Manfred, W., Brett, Y., Jost, H., Alfred, W., Douglas, O., Frank, S., Paolo, L., Loretta, R.: Droplet Formation and Growth in Polluted Fogs, *Contr. Atmos. Phys.*, **71** (1), 65-85 (1998).
3. Itahashi, S., Uchida, R., Yamaji, K., Chatani, S.: Year-round modeling of sulfate aerosol over Asia through updates of aqueous-phase oxidation and gas-phase reactions with stabilized Criegee intermediates, *Atmos. Environ. X*, 12, 100123, doi:10.1016/j.aeaoa.2021.100123 (2021).
4. Itahashi, S., Hattori, S., Ito, A., Sadanaga, Y., Yoshida, N., Matsuki, A.: Role of dust and iron solubility in sulfate formation during the long-range transport in East Asia evidenced by ^{17}O-excess signatures, Environ. Sci. Tech., 56, 13634–13643, doi: 10.1021/acs.est.2c03574 (2022).
5. Itahashi, S. Hatakeyama, S., Shimada, K., Takami, A.: Sources of high sulfate aerosol concentration observed at Cape Hedo in spring 2021, Aerosol and Air Quality Research, 19, 587–600, doi:10.4209/aaqr.2018.09.0350 (2019).
6. Itahashi, S., Kim, N. K., Kim, Y. P., Song, M., Kim, C. H., Jang, K. S., Lee, K. Y., Shin, H. J., Ahn, J. Y., Jung, J. S., Wu, Z., Lee, J. Y., Sadanaga, Y., Kato, S., Tang, N.,
7. Matsuki, A.: Distinctive features of inorganic $PM_{1.0}$ components during winter pollution events over the upwind and downwind regions in Northeast Asia. *Atmos. Environ.*, 309, 119943 (2023).
8. Japan Meteorological Agency: Activity status of each volcano, http://www.data.jma.go.jp/svd/vois/data/tokyo/volcano.html (accessed 9 January 2024) (in Japanese)
9. Kajino, M., Hagino, H., Fujitani, Y., Morikawa, T., Fukui, T., Onishi, K., Okuda, T., Kajikawa, T., Igarashi Y.: Modeling transition metals in East Asia and Japan and its emission sources, *GeoHealth*, 4, e2020GH000259, doi:10.1029/2020GH000259, (2020).
10. Kaneyasu, N., Igarashi, Y., Sawa, Y., Takahashi, H., Takada, H., Kumata, H., Hoeller, R.: Chemical and optical properties of 2003 Siberian forest fire smoke observed at the summit of Mt. Fuji, Japan. *J. Geophys. Res.,* **112** (D13) (2007).

11. Kato, S., Shiobara, Y., Uchiyama, K., Miura, K., Okochi, H., Kobayashi, H., Hatakeyama, S.: Atmospheric CO, O_3, and SO_2 Measurements at the Summit of Mt. Fuji during the Summer of 2013, *Aerosol Air Qual. Res.*, **16** (10), 2368-2377 (2016).
12. Kevin, J. N., John, A. O., Anneli, H.: Elemental composition of fog interstitial particle size fractions and hydrophobic fractions related to fog droplet nucleation scavenging, *Tellus*, **44B**, 593-603 (1992).
13. Kocak, M., Mihalopoulos, N., and Kubilay, N.: Chemical composition of the fine and coarse fraction of aerosols in the northeastern Mediterranean, *Atmos. Environ.*, **41**, 7351–7368. doi:10.1016/j.atmosenv.2007.05.011 (2007).
14. Li, J., Posfai, M., Hobbs, P.V. and Buseck, P. R.: Individual aerosol particles from biomass burning in southern Africa: 2, Compositions and aging of inorganic particles, *J. Geophys. Res.*, **108**, 8484 (2003).
15. Miura, K., Shimada, K., Sugiyama, T., Sato, K., Takami, A., Chan, C.K., Kim, I.S., Kim, Y. P., Lin, N.-H., Hatakeyama, S., 2019. Seasonal and annual changes in PAH concentrations in a remote site in the Pacific Ocean. Sci. Rep. 9, 12591.
16. Naoe, H., Heintzenberg, J., Okada, K., Zaizen, Y., Hayashi, K., Tateishi, T., Igarashi, Y., Dokiya, Y., Kinoshita, K.: Composition and size distribution of submicrometer aerosol particles observed on Mt. Fuji in the volcanic plumes from Miyakejima. *Atmos. Environ.*, **37** (22), 3047-3055 (2003).
17. Okamoto, S., Tanimoto, H.: A review of atmospheric chemistry observations at mountain sites. *Prog. Earth Planet. Sci.,,* **3** (1), 34 (2016).
18. Okuda, T., Nakao, S., Tanaka, S., Shen, Z., He, K., Ma, Y., Lei, Y., Jia, Y.: Characterization of water-soluble ionic composition of aerosols in Xi'an and Beijing, China. *Chikyukagaku (Geochemistry)*, **41**, 113-123. (in Japanese with English abstract) (2007).
19. Osada, K., Ohara, T., Uno, I., Kido, M., Iida, H.: Impact of Chinese anthropogenic emissions on submicrometer aerosol concentration at Mt. Tateyama, Japan. *Atmos. Chem. Phys.*, **9** (23), 9111-9120 (2009).
20. Otani, Y., Eryu, K., Furuuchi, M., Tajima, N., & Tekasakul, P.: Inertial classification of nanoparticles with fibrous filters. *Aerosol and Air Qual. Res,* **7**, 343-352 (2007).
21. Parmar, R. S., Satsangi, G. S., Kumari, M., Lakhani, A., Srivastava, S. S., Prakash, S.: Study of size distribution of atmospheric aerosol at Agra, *Atmos. Environ.*, **35**,

693–702. doi:10.1016/S1352-2310(00)00317-4 (2001).
22. Shimada, K., Geka, Y., Kato, S., Chan, C. K., Kim, Y. P., Ou-Yang, C. F., Lin, N-H., Hatakeyama, S.: Possibility of condensation of nitric acid for cloud condensation nucleus in the summer at Mt. Fuji, *Atmos. Pollut. Res.*, 15(1), 101940 (2024).
23. Shimada, K., Mizukoshi, M., Chan, C. K., Kim, Y. P., Lin, N. H., Matsuda, K., Itahashi, S., Yoshihiro Nakashima, Hatakeyama, S.: Disentangling the contribution of the transboundary out-flow from the Asian continent to Tokyo, Japan, *Environ. Pollut,* 286, 117280 (2021).
24. Shimada, K., Shimada, M., Takami, A., Hasegawa, S., Fushimi, A., Arakaki, T., Watanabe, I., Hatakeyama, S.: Mode and Place of Origin of Carbonaceous Aerosols Transported From East Asia to Cape Hedo, Okinawa, Japan, *Aerosol and Air Qual. Res,* **15***,* 799-813 (2015).
25. Suzuki, I., Igarashi, Y., Dokiya, Y., Akagi, T.: Two extreme types of mixing of dust with urban aerosols observed in Kosa particles: 'after' mixing and 'on-the-way' mixing. *Atmos. Environ.*, **44** (6), 858-866 (2010).
26. Stein, A.F., Draxler, R.R, Rolph, G.D., Stunder, B.J.B., Cohen, M.D., Ngan, F.: NOAA's HYSPLIT atmospheric transport and dispersion modeling system, Bull. Amer. Meteor. Soc., 96, 2059-2077, (2015). http://dx.doi.org/10.1175/BAMS-D-14-00110.1
27. Takami, A., Miyoshi, T., Shimono, A., Kaneyasu, N., Kato, S., Kajii, Y., Hatakeyama, S.: Transport of anthropogenic aerosols from Asia and subsequent chemical transformation, *J. Geophys. Res.*, **112**, D22S31. doi:10.1029/2006JD008120 (2007).
28. Taniguchi, Y., Shimada, K., Takami, A., Lin, N. H., Chan, C. K., Kim, Y. P., Hatakeyama, S.: Transboundary and local air pollutants in western Japan distinguished on the basis of ratios of metallic elements in size-segregated aerosols, *Aerosol and Air Qual. Res,* **17**, 3141-3150. (2017).
29. Taylor, S. R., Mclennan, S. M.: The Geochemical Evolution of the Continental Crust. *Rev Geophys.,* **33**, 241-265 (1995).
30. U.S. Environmental Protection Agency: CMAQ (Version 5.3.3), https://doi.org/10.5281/zenodo.5213949 (2021) (accessed 9 January 2024).
31. Wai, K. M., Lin, N. H., Wang, S. H., Dokiya, Y.: Rainwater chemistry at a high‐altitude station, Mt. Lulin, Taiwan: Comparison with a background station, Mt. Fuji.

*J. Geophys. Res.,***113** (D6) (2008).
32. Xiaoxiu, L., Xiaoshan, Z., Yujing, M., Anpu, N., Guibin, J.: Size fractionated speciation of sulfate and nitrate in airborne particulates in Beijing, China, *Atmos. Environ.*, **37**, 2581–2588. doi:10.1016/S1352-2310(03)00220-6 (2003).
33. Xie, Y., Paulot, F., Carter, W. P. L., Nolte, C. G., Luecken, D. J., Hutzell, W. T., Wennberg, P. O., Cohen, R. C., and Pinder, R. W.: Understanding the impact of recent advances in isoprene photooxidation on simulations of regional air quality, *Atmos. Chem. Phys.*, 13, 8439–8455, doi:10.5194/acp-13-8439-2013 (2013).
34. Xu, L., Pye, H. O. T., He, J., Chen, Y., Murphy, B. N., and Ng, N. L.: Experimental and model estimates of the contributions from biogenic monoterpenes and sesquiterpenes to secondary organic aerosol in the southeastern United States, *Atmos. Chem. Phys.*, 18, 12613–12637, doi:10.5194/acp-18-12613-2018 (2018).
35. Yeatman, S., Spokes, L., Jickells, T.: Comparisons of coarse-mode aerosol nitrate and ammonium at two polluted coastal sites, *Atmos. Environ.*, **35**, 1321–1335. doi:10.1016/S1352-2310(00)00452-0 (2001).
36. Yumoto, Y., Shimada, K., Araki, Y., Yoshino, A., Takami, A., Hatakayema, S.: Size-segregated Chemical Analyses of Particles Transported from East Asia to Cape Hedo, Okinawa and Their Transformation Mechanisms during the Transport, *Earozoru Kenkyu*, **30**, 115-125 (2015). (in Japanese with English Abstract).
37. Zhuang, H., Chan, C. K., Fang, M., Wexler, A. S.: Formation of nitrate and non-sea-salt sulfate on coarse particles, *Atmos. Environ.*, **33**, 4223–4233. doi:10.1016/S1352-2310(99)00186-7 (1999).

Figure Captions

Fig. 1 Size segregated mass concentrations in the first and the second periods.

Fig. 2 Spatial distribution of the simulated sulfate concentration without volcano and including volcano emission, and of the difference in volcanic emissions during the first and the second periods.

Fig. 3 Size segregated ionic concentrations in the first and the second periods.

Fig. 4 Size segregated element concentrations in the first and the second periods.

Fig. 5 (a)Scatter plot of nss-SO_4^{2-} against NH_4^+. (b)Scatter plot of nss-SO_4^{2-} against NH_4^+ + infer-H^+

Fig. 6 Size segregated sulfate concentrations in Tokyo and Okinawa.

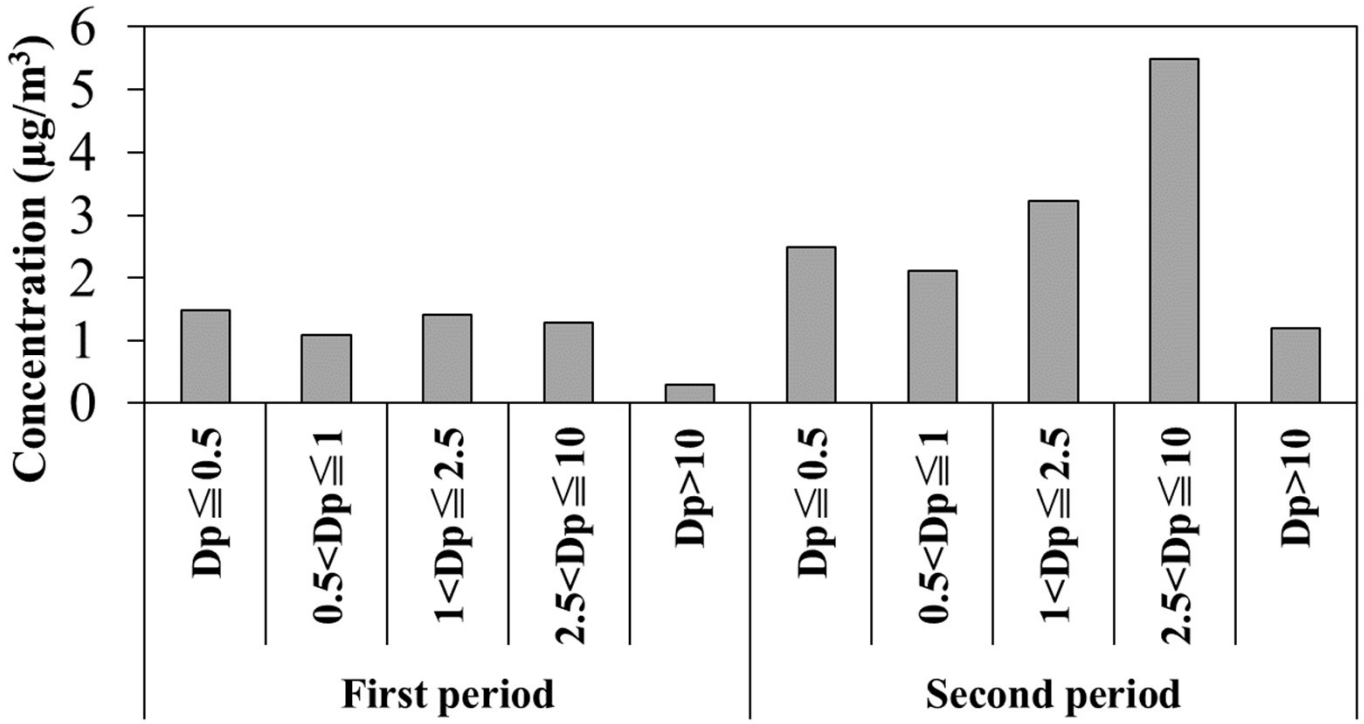
Concentration (μg/m³)
6
5
4
3
2
1
0
Dp≦0.5
0.5<Dp≦1
1<Dp≦2.5
2.5<Dp≦10
Dp>10
Dp≦0.5
0.5<Dp≦1
1<Dp≦2.5
2.5<Dp≦10
Dp>10
First period
Second period

Fig. 1

Fig. 2

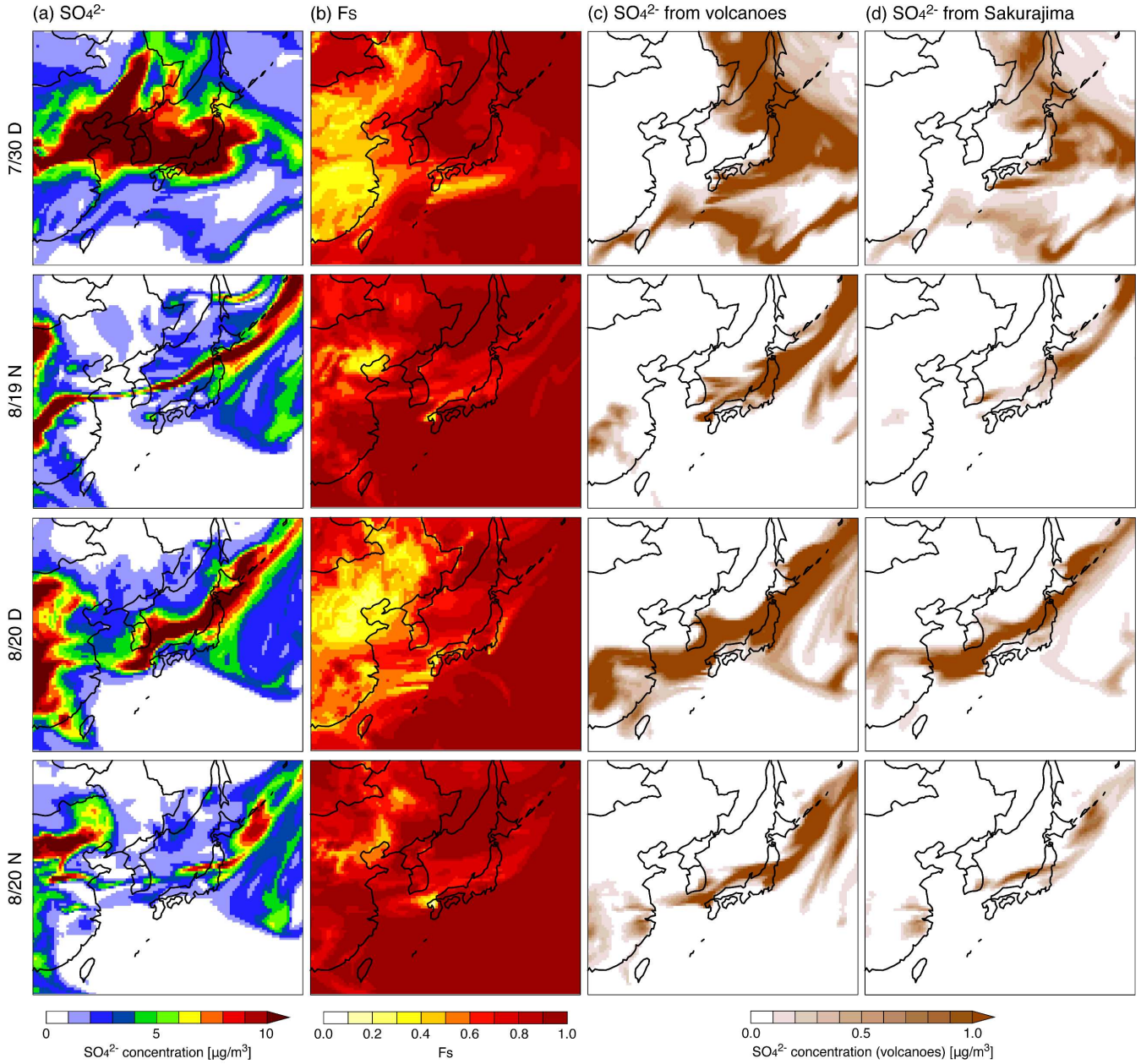
(a) SO4 2-
(b) Fs
(c) SO4 2- from volcanoes
(d) SO4 2- from Sakurajima
7/30 D
8/19 N
8/20 D
8/20 N
0
5
10
SO4 2- concentration [μg/m3]
0.0
0.2
0.4
0.6
0.8
1.0
Fs
0.0
0.5
1.0
SO4 2- concentration (volcanoes) [μg/m3]

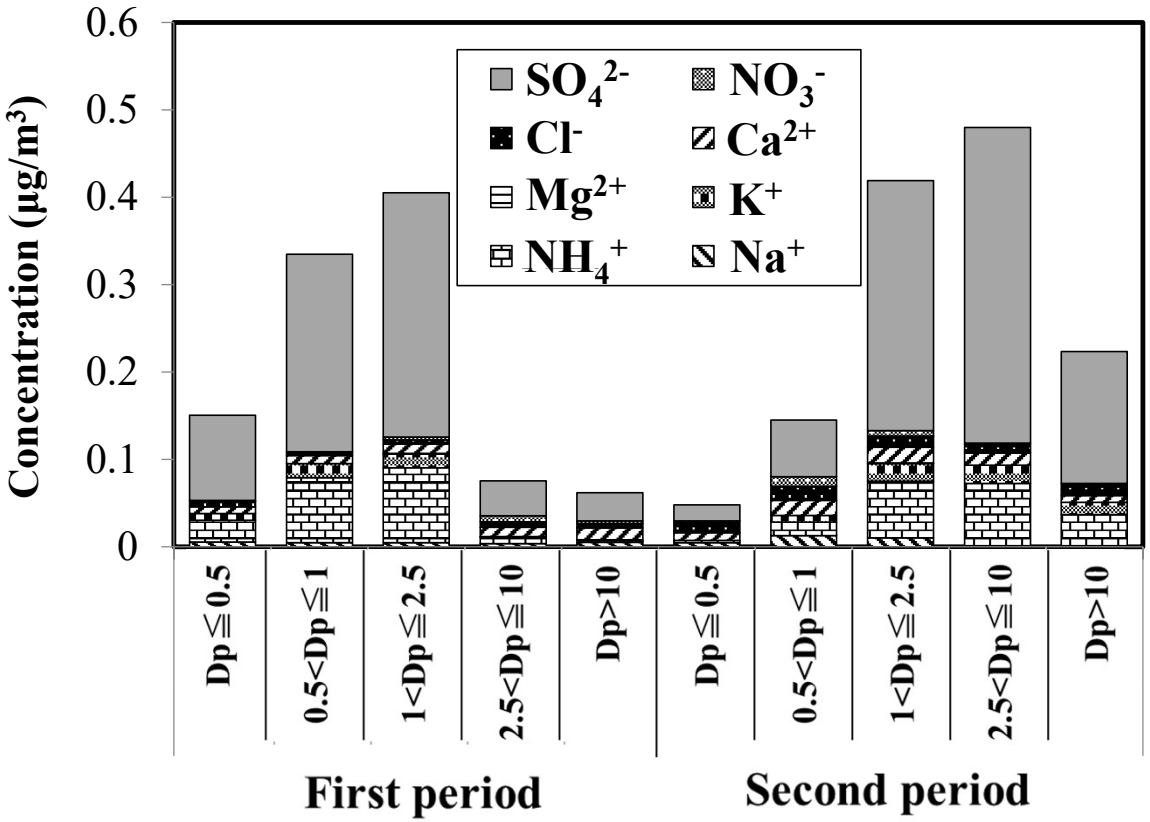
Concentration (μg/m³)
0.6
0.5
0.4
0.3
0.2
0.1
0
SO4 2-
NO3 -
Cl-
Ca2+
Mg2+
K+
NH4 +
Na+
Dp≦0.5
0.5<Dp≦1
1<Dp≦2.5
2.5<Dp≦10
Dp>10
Dp≦0.5
0.5<Dp≦1
1<Dp≦2.5
2.5<Dp≦10
Dp>10
First period
Second period

Fig. 3

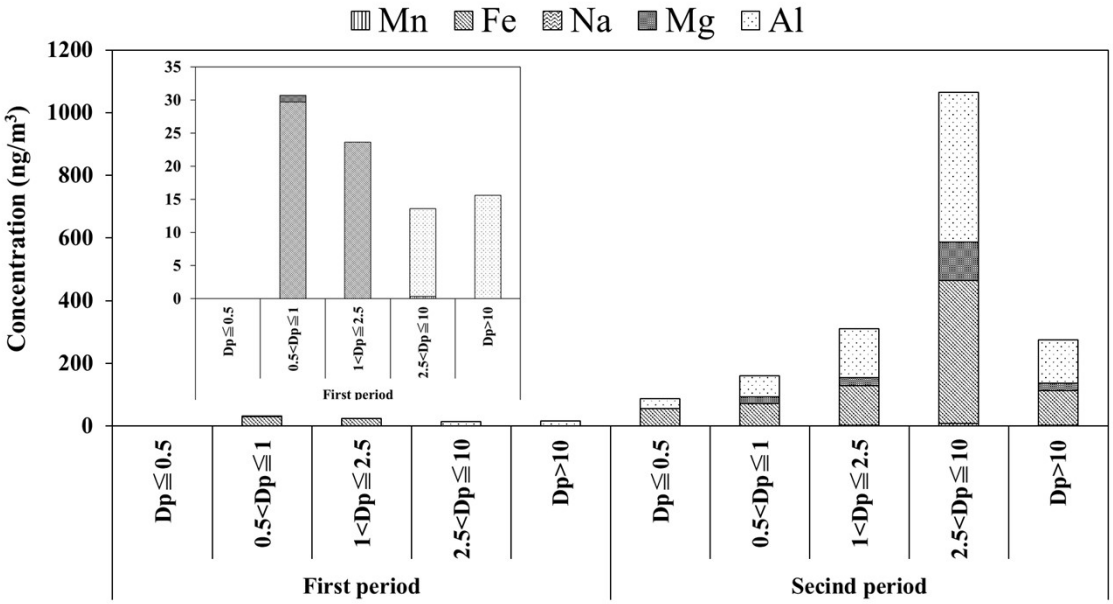
Mn
Fe
Na
Mg
Al
Concentration (ng/m3)
1200
1000
800
600
400
200
0
35
30
25
20
15
10
5
0
Dp≦0.5
0.5<Dp≦1
1<Dp≦2.5
2.5<Dp≦10
Dp>10
First period
Dp≦0.5
0.5<Dp≦1
1<Dp≦2.5
2.5<Dp≦10
Dp>10
Dp≦0.5
0.5<Dp≦1
1<Dp≦2.5
2.5<Dp≦10
Dp>10
First period
Secind period

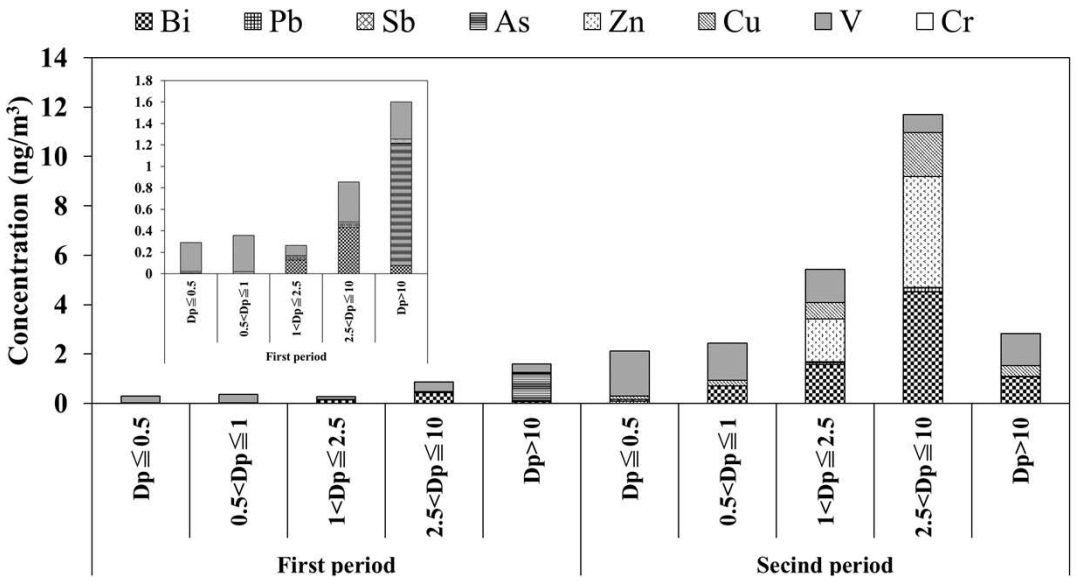
Bi
Pb
Sb
As
Zn
Cu
V
Cr
Concentration (ng/m3)
14
12
10
8
6
4
2
0
1.8
1.6
1.4
1.2
1
0.8
0.6
0.4
0.2
0
Dp≦0.5
0.5<Dp≦1
1<Dp≦2.5
2.5<Dp≦10
Dp>10
First period
Dp≦0.5
0.5<Dp≦1
1<Dp≦2.5
2.5<Dp≦10
Dp>10
Dp≦0.5
0.5<Dp≦1
1<Dp≦2.5
2.5<Dp≦10
Dp>10
First period
Secind period

Fig. 4

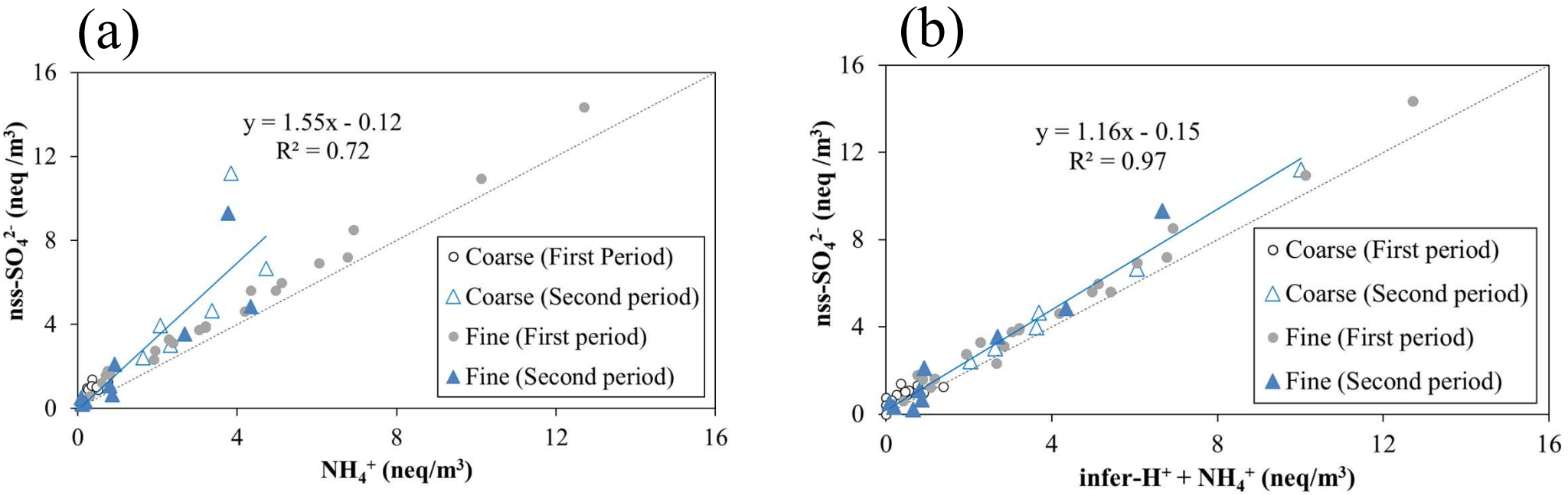
(a)
y = 1.55x - 0.12
R² = 0.72
Coarse (First Period)
Coarse (Second period)
Fine (First period)
Fine (Second period)
nss-SO4 2- (neq /m3)
NH4+ (neq/m3)
0
4
8
12
16
(b)
y = 1.16x - 0.15
R² = 0.97
Coarse (First period)
Coarse (Second period)
Fine (First period)
Fine (Second period)
nss-SO4 2- (neq /m3)
infer-H+ + NH4+ (neq/m3)

Fig. 5

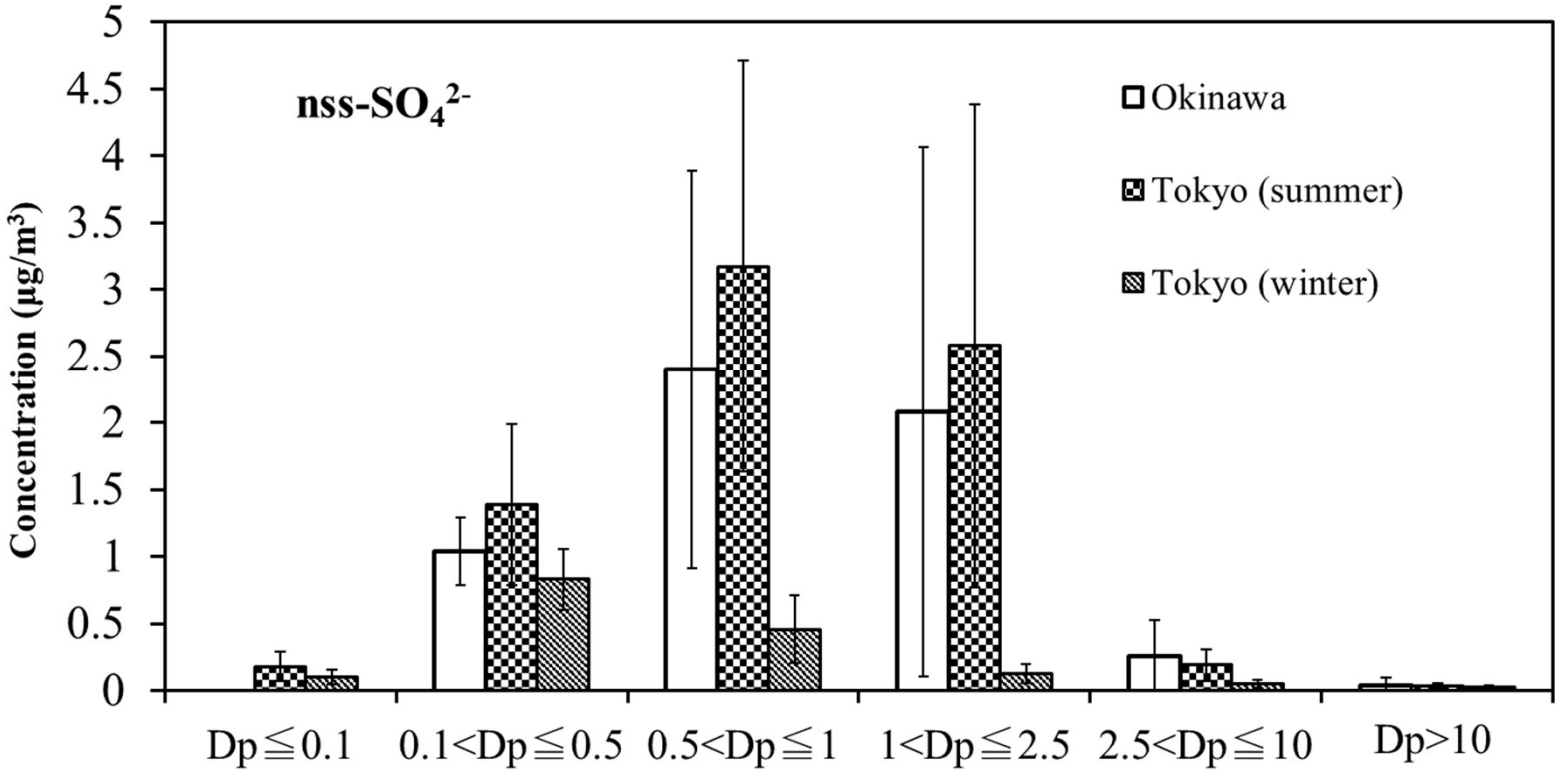
nss-SO4 2-
Okinawa
Tokyo (summer)
Tokyo (winter)
Concentration (μg/m3)
5
4.5
4
3.5
3
2.5
2
1.5
1
0.5
0
Dp≦0.1
0.1<Dp≦0.5
0.5<Dp≦1
1<Dp≦2.5
2.5<Dp≦10
Dp>10

Fig. 6